

TABLE I. Pair-correlation function at contact.

$\rho\sigma^2$	a	$g(\sigma)$	$g(\sigma)^a$
0.1	1.086	1.137	1.14
0.2	1.181	1.307	1.31
0.3	1.275	1.524	1.52
0.4	1.366	1.805	1.80
0.5	1.451	2.179	2.18
0.6	1.532	2.693	2.70
0.7	1.608	3.433	3.45
0.8	1.680	4.568	4.61
0.9	1.749	6.478	6.55

* Numerical solution of the PY equation (Ref. 6).

$S'(r) = 1$ exactly and $c(r)$ is determined by Eq. (3), where $c(0)$ and $c(1)$ can be calculated from Eq. (4) and Eq. (3) for $r = 1$.

A simple Ansatz for $S'(r)$ is

$$S'(r) = (1 - a^2 r^2 / 4)^{d-1/2} \quad (5)$$

which is exact not only in one but also in three dimensions. Furthermore, in the low density limit, if $a = 1$, the Ansatz is exact for all d . The pressure of the fluid is related to the pair distribution function at contact $g(1) = -c(1)$ by the virial theorem $P/\rho k_B T = 1 + \rho V_d \cdot g(1)/2$. In odd dimensions the pressure, as given by the PY approximation, diverges at the packing fraction $\eta = \rho V_d / 2^d = 1$. Assuming this to be the case also in even dimensions the Ansatz (5) is exact in the high density limit $\eta \rightarrow 1$ for all d also, if $a = 2$. For $d > 1$ the parameter a can be determined by calculating the third derivative of $c(r)$ at $r = 0$ yielding

$$S'''(0) = -\frac{d-1}{4} - \frac{2}{d+1} \times \{ [c'(1)]^2 - 2c(1)c''(1) - (d-1)c(1)c'(1) \} / c^2(1). \quad (6)$$

For $d = 3$, solving Eqs. (6), (4), and (3) for $r = 1$, one finds the exact result $a(\eta) = (1 + 2\eta)/(1 + \eta/2)$. For $d = 2$, integration of Eq. (5) yields

$$S(r) = \left\{ \arcsin\left(\frac{ar}{2}\right) + \frac{ar}{2} \left[1 - \left(\frac{ar}{2}\right)^2 \right]^{1/2} \right\} / a. \quad (7)$$

Solving Eqs. (6), (4), and (3) for $r = 1$ the parameter a is found

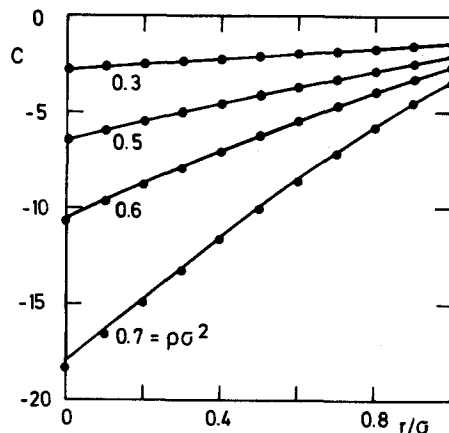


FIG. 1. Direct correlation function $c(r)$ for various densities $\rho\sigma^2$. The dots are the numerical solution to the PY equation.

to increase monotonously from $a = 1$ at $\eta = 0$ to $a = 2$ at $\eta = 1$. As can be seen from Table I the resulting pair correlation function at contact $g(1)$ is in good agreement with the numerical exact solution to the PY equation.⁶ Also, in the high density limit, $\eta \rightarrow 1$, the Ansatz (5) implies that $g(1)$ diverges as $(1 - \eta)^{-(d+1)/2}$ which is consistent with known results in odd dimensions.⁵

Although the Ansatz (5) does not reproduce the next to leading term in the virial expansion of $S'(r)$ exactly, which is expressible by elliptic integrals in even dimensions, the resulting direct correlation function is a good approximation to the numerical exact solution of the PY equation in the whole density regime as is demonstrated in Fig. 1. Thus the simple analytical expressions (3) and (7) for the direct correlation function $c(r)$ of a hard disk fluid may be helpful in applications involving the structure of two-dimensional systems.

¹J. K. Percus and G. J. Yevick, Phys. Rev. **110**, 1 (1958).

²J. A. Barker and D. Henderson, Rev. Mod. Phys. **48**, 587 (1976).

³M. S. Wertheim, J. Math. Phys. **5**, 643 (1964).

⁴M. S. Wertheim, Phys. Rev. Lett. **10**, 321 (1963); E. Thiele, J. Chem. Phys. **39**, 474 (1963).

⁵E. Leutheusser, Physica A **127**, 667 (1984).

⁶F. Lado, J. Chem. Phys. **49**, 3092 (1968).

Negative ion photoelectron spectroscopy of TeH^-

C. B. Freidhoff, J. T. Snodgrass, J. V. Coe, K. M. McHugh, and K. H. Bowen
Department of Chemistry, The Johns Hopkins University, Baltimore, Maryland 21218

(Received 3 September 1985; accepted 9 October 1985)

The tellurium hydride diatomic radical has been studied by paramagnetic resonance,¹ by flash photolysis with flash spectroscopy in the ultraviolet,^{2,3} and indirectly by electron impact ionization⁴ of H_2Te to yield HTe^+ . Here, we report

the recording of the photodetachment spectrum of TeH^- by negative ion photoelectron spectroscopy. In the past, photodetachment spectroscopies have been employed by several investigators⁵⁻⁷ to study the electronically analogous nega-

tive ion hydrides OH^- , SH^- , and SeH^- . Our work on TeH^- adds a fourth ion to the list of diatomic group VI B hydride negative ions which have been studied by photodetachment techniques.

In negative ion photoelectron spectroscopy a mass-selected negative ion beam is crossed with a fixed-frequency laser beam, and the resulting photodetached electrons are subjected to energy analysis. Our apparatus, which has been described previously,⁸ employs a Wien velocity filter for mass selection, an argon ion laser operated intracavity in the ion-photon interaction region, and a magnetically shielded, hemispherical electron energy analyzer. The ion source used in this work was a cold cathode Penning discharge source of the type originally developed by Heinicke *et al.*⁹ This source consists of a cylindrical anode, two button cathodes located near opposite ends of the anode, an oven for supplying vapors to the anode, and an electromagnet for generating a magnetic field along the axis of the anode cylinder. Negative ions were extracted radially through an aperture in the side of the anode into the photoelectron spectrometer. To generate tellurium-containing negative ions, elemental tellurium was heated in the oven to $\sim 500^\circ\text{C}$ to provide ~ 1 Torr of vapor pressure to the anode, and argon was added as the discharge support gas. Mass spectra of the negative ions produced in this fashion showed the presence of $\text{Te}_{n=1-7}^-$, TeO^- , and TeO_2^- . TeH^- was concealed by Te^- in these mass spectra both because of our available mass resolution and because it was masked by the wide isotopic pattern of tellurium. Since Te^- and TeH^- were not separated from one another by our mass selector, they were photodetached simultaneously in the photoelectron spectrometer thereby revealing the presence of TeH^- spectroscopically. The Penning source has a propensity for forming oxide and hydride negative ions even when there is no evident supply of oxygen or hydrogen available. We suspect that water baked off the oven and the discharge electrodes may be the source of the necessary ingredients.

A photoelectron spectrum recorded with 2.540 eV photons and containing both the well-known spectrum of Te^- and the heretofore unknown spectrum of TeH^- is presented in Fig. 1. Under peaks A and B reside the atomic photodetachment transitions¹⁰ of Te^- . Peak C is the sole spectral feature in this spectrum corresponding to TeH^- ($\text{TeH}^-, X^1\Sigma^+ \rightarrow \text{TeH}, X^2\Pi_{3/2}$). Several such photoelectron spectra were recorded with the mass selector alternately tuned to the low, the middle, and the high mass sides of the unresolved Te^-/TeH^- mass peak. While the ratio of the height of peak A to that of peak B remained constant at all three mass positions, the ratio of the height of peak C to that of peak A (or B) was largest on the high mass side and lowest on the low mass side. This is consistent with peak C deriving from a negative ion species with the same wide isotope pattern as Te^- but with a slightly higher mass. Furthermore, the addition of H_2 gas into the source had the effect of increasing the ratio of peak C to peak B (or A) by as much as a factor of 2.

The photoelectron spectrum of TeH^- (peak C) is self-calibrated by the Te^- transitions in the same spectrum and these also provide an energy scale compression factor of 1.026 and an electronic temperature for ions produced in

this source of 1700 ± 200 K if a Boltzmann distribution is assumed. The adiabatic electron affinity of TeH was calculated from the following equation:

$$\text{E.A.}(\text{TeH}) = \text{E.A.}(\text{Te}) + \gamma[\Omega(\text{Te}^-) - \Omega(\text{TeH}^-)] + mW \left[\frac{1}{M(\text{Te})} - \frac{1}{M(\text{TeH})} \right], \quad (1)$$

where $\text{E.A.}(\text{Te})$ is the electron affinity of tellurium, γ is the energy scale compression factor, $\Omega(\text{Te}^-)$ is the laboratory electron kinetic energy position for the $\text{Te}^-, ^2P_{3/2} \rightarrow \text{Te}, ^3P_2$ transition, $\Omega(\text{TeH}^-)$ is the laboratory electron energy for the TeH^- transition, m is the mass of an electron, W is the beam energy (500 eV), and $M(\text{Te})$ and $M(\text{TeH})$ are the respective masses of Te and TeH. From this the electron affinity of TeH was found to be 2.102 ± 0.015 eV. Using this determination in conjunction with the dissociation energy for TeH reported by Balkis *et al.*⁴ gives an estimate for the dissociation energy of TeH^- into Te^- and H of 2.0 eV.

The formation of the negative ions of the group VI B diatomic hydrides is thought to involve the addition of electrons into nonbonding orbitals of the neutral hydrides. Photodetachment studies of OH^- , SH^- , and SeH^- indicate that the structures of these negative ions are very close to those of their corresponding neutrals.⁵⁻⁷ The single peak observed in our photoelectron spectrum of TeH^- leads to the same conclusion. As predicted by Cade,¹¹ the magnitudes of the electron affinities of the group VI B diatomic hydrides are closer to those of their constituent group VI B atoms than they are

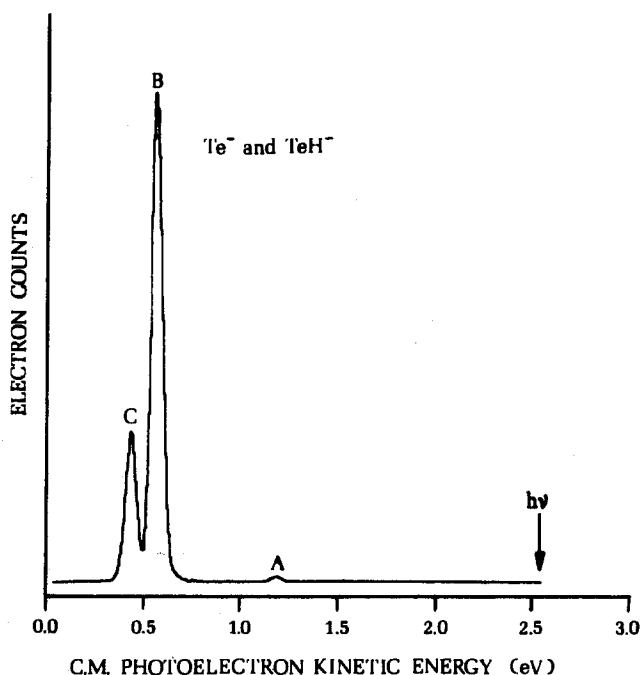


FIG. 1. The photoelectron spectrum of Te^- and TeH^- recorded simultaneously with 2.540 eV photons and presented in terms of center of mass (c.m.) electron kinetic energies. Peak A corresponds to the $\text{Te}^-, ^2P_{1/2} \rightarrow \text{Te}, ^3P_2$ transition. Under peak B reside the $\text{Te}^-, ^2P_{1/2} \rightarrow \text{Te}, ^3P_0, ^3P_1$, and the $\text{Te}^-, ^2P_{3/2} \rightarrow \text{Te}, ^3P_2$ transitions. Peak C corresponds to the $\text{TeH}^-, X^1\Sigma^+ \rightarrow \text{TeH}, X^2\Pi_{3/2}$ transition. The $\text{TeH}^-, X^1\Sigma^+ \rightarrow \text{TeH}, X^2\Pi_{1/2}$ transition is energetically inaccessible in this spectrum (Ref. 3).

TABLE I. Electron affinities (eV) of the group VI B atoms, their diatomic hydrides, and the halogen atoms.

Group VI B atoms (Ref. 12)		Group VI B hydrides (Ref. 13)		Halogen atoms (Ref. 12)	
O	(1.462)	OH	(1.828)	F	(3.399)
S	(2.077)	SH	(2.317)	Cl	(3.615)
Se	(2.021)	SeH	(2.21)	Br	(3.364)
Te	(1.971)	TeH	(2.102)	I	(3.059)

to those of their halogen atom isoelectronic analogs. The hydride electron affinities also approach those of their group VI B atoms more closely as one proceeds to the heavier species. Table I summarizes these periodic trends. Each of its columns exhibits the same pattern in which the electron affinity increases in going from the first to the second rows and then decreases in going to the third and fourth rows. The electron affinity of TeH determined in this work fits nicely into these periodic trends.

This research was supported in part by the Research Corporation. Acknowledgment is also made to the Donors of The Petroleum Research Fund, administered by the American Chemical Society, for partial support of this research.

¹H. E. Radford, *J. Chem. Phys.* **40**, 2732 (1964).

²R. J. Donovan, D. J. Little, and J. Konstantatos, *J. Chem. Soc. Faraday Trans. 2* **68**, 1812 (1972).

³D. J. Little, R. J. Donovan, and R. J. Butcher, *J. Photochem.* **2**, 451 (1974).

⁴T. Balkis, A. F. Gaines, G. Ozgen, I. T. Ozgen, and M. C. Flowers, *J. Chem. Soc. Faraday Trans. 2* **72**, 524 (1976).

⁵P. A. Schulz, R. D. Mead, P. L. Jones, and W. C. Lineberger, *J. Chem. Phys.* **77**, 1153 (1982).

⁶F. Breyer, P. Frey, and H. Hotop, *Z. Phys. A* **300**, 7 (1981).

⁷K. C. Smyth and J. I. Brauman, *J. Chem. Phys.* **56**, 5993 (1972).

⁸J. V. Coe, J. T. Snodgrass, C. B. Freidhoff, K. M. McHugh, and K. H. Bowen, *J. Chem. Phys.* **83**, 3169 (1985).

⁹E. Heinicke, K. Bethge, and H. Baumann, *Nucl. Instrum. Methods* **58**, 125 (1968).

¹⁰J. Slater and W. C. Lineberger, *Phys. Rev. A* **15**, 2277 (1977).

¹¹P. E. Cade, *Proc. Phys. Soc.* **91**, 842 (1967).

¹²R. D. Mead, A. E. Stevens, and W. C. Lineberger, in *Gas-Phase Ion Chemistry*, edited by M. T. Bowers (Academic, New York, 1984), Vol. 3.

¹³P. S. Drzaic, J. Marks, and J. I. Brauman, in *Gas-Phase Ion Chemistry*, edited by M. T. Bowers (Academic, New York, 1984), Vol. 3. Except for E.A.(TeH) which was determined in this work.

Multiphoton ionization spectra of *trans*-1,3-butadiene: Reassignment of a Rydberg series

Philip H. Taylor, W. Gary Mallard, and Kermit C. Smyth

Center for Fire Research, National Bureau of Standards, Gaithersburg, Maryland 20899

(Received 16 July 1985; accepted 2 October 1985)

A new Rydberg series of *trans*-1,3-butadiene has been recently observed using two-photon resonant, three-photon ionization in the 330–269 nm wavelength region.¹ The rate-limiting step in the multiphoton ionization process is the two-photon transition from the ground state. For this transition, either an *s* or a *d* final state is optically allowed. An *ns* assignment was originally made due to the spectral similarity of the proposed 4*s* and 5*s* origins and associated vibronic structure with that of the 3*s* origin region.² Subsequently, we have learned that the same Rydberg series has been observed by Otis and Whetten and that their results on the polarization behavior are not consistent with an *s* series assignment.³ Therefore, we have reexamined the butadiene multiphoton ionization spectrum using both linearly and circularly polarized light.

The theoretical basis for classifying the symmetry of electronic states based on the polarization dependence of their two-photon transition rates has been developed by Monson and McClain⁴ and generalized by McClain.⁵ Nascimento has extended the theory to open shell molecules and

provided a simple set of rules for any two-photon transition in the case of randomly oriented molecules.⁶ These rules can be expressed in terms of the ratio of the two-photon transition rate for excitation due to circularly polarized light to that for excitation due to linearly polarized light, $\Omega = \sigma_{\text{circular}}/\sigma_{\text{linear}}$. The results may be summarized as (1) $\Omega < 1$ for transitions between states of the same symmetry and (2) $\Omega = 3/2$ for transitions between states of different symmetry. Thus a study of the ratio of the ionization signal for circular vs linear polarization should provide information on the symmetry of the Rydberg states.

The *trans*-1,3-butadiene molecule belongs to the C_{2h} symmetry group, and its ground state electronic configuration is of A_g symmetry. Since the observed limit of this Rydberg series is the lowest ionization potential of butadiene,¹ the excitation must be from the highest occupied molecular orbital (orbital symmetry b_g). For an electron promoted to an *ns* Rydberg orbital, the resulting symmetry of the excited state is B_g . For an electron promoted to an *nd* Rydberg orbital, the symmetry of the excited state is either A_g for the *nd π*

The Journal of Chemical Physics is copyrighted by the American Institute of Physics (AIP). Redistribution of journal material is subject to the AIP online journal license and/or AIP copyright. For more information, see <http://ojps.aip.org/jcpo/jcpcr/jsp>
Copyright of Journal of Chemical Physics is the property of American Institute of Physics and its content may not be copied or emailed to multiple sites or posted to a listserv without the copyright holder's express written permission. However, users may print, download, or email articles for individual use.